A COMPARATIVE STUDY ON THE EFFECT OF USING CONVENTIONAL AND HIGH PRESSURE GRINDING ROLLS CRUSHING ON THE BALL MILL GRINDING KINETICS OF AN IRON ORE

Kianoush BARANI, Hossein BALOCHI

Department of Mining Engineering, Lorestan University, Khorramabad, Iran, barani.k@lu.ac.ir

Abstract: The effect of using conventional and high pressure grinding rolls (HPGR) crushing on the ball mill grinding of an iron ore was assessed to determine how these different comminution processes affect the ball mill grinding kinetic. For this purpose, the sample was obtained from the Jalalabad Iron Ore Mine and crushed by conventional crusher and HPGR. Then, the crushing products were ground in a laboratory ball mill. Five single-sized fractions of (–4+3.15 mm), (–2+1.7 mm), (–1+0.850 mm), (–0.500+0.420 mm), and (–0.212+0.180 mm) were selected as the ball mill feed. The specific rates of breakage (S_i) and cumulative breakage distribution function ($B_{i,j}$) values were determined for those size fractions. It was found that for all fraction the $B_{i,1}$ values of the HPGR product were higher than those for the crusher product. It means that the particles produced by the dry ball milling of the HPGR product were finer than by the crusher. Also, the results showed that the specific breakage rate of the material crushed by HPGR at coarse fractions (–4+3.15 mm, -2+1.7 mm, and -1+0.850 mm) was higher than the material crushed by conventional crushers. However, at fine fractions (–0.500+0.420 mm and -0.212+0.180 mm), there was a small difference and the specific breakage rates were the same. This issue can be explained by the fact, that for coarse fractions the particles had longer side surfaces and thus were more affected by the lateral pressure. The results of verification test showed that after 60 seconds of grinding the 80% passing size of the HPGR and crusher products (D_{80}) were reduced from 3311 μm to 760 μm and 1267 μm, respectively.

Introduction

Schonert (1979) showed that the most energy-efficient method of comminuting particles is to compress them between two plates. Compressing a particle bed between two counter rotating rolls was achieved by the invention of high pressure grinding rolls (HPGR) (Schonert and Knobloch, 1984). The first commercial application of

HPGR was in 1985 and its success resulted in the increasing numbers of applications in the cement, iron ore, and diamond industries (Kellerwessel, 1990).

The comminution principle, which is a compression as a breakage mechanism used in the HPGR, is different from the one in conventional crushers or tumbling mills where impact and abrasion breakage mechanisms are dominant. In the HPGR, contrary to the conventional crushing rolls, the particles are broken by compression in a packed particle bed, not by direct nipping of the particles between two rolls. This particle bed is created between two choke-fed, counter-rotating rolls. Between these rolls, a particle bed is pressed to the density of roughly up to 85% of the actual material density (Schonert, 1988; Aydogan et al., 2006; Schneider et al., 2009). This type of crushing causes micro-cracking along grain boundaries and preferential liberation of valuable minerals (Dunne et al., 1996; Bearman, 2006; Klymowsky et al., 2006; Morley, 2006; Daniel, 2007). As a result, the product from a HPGR is different and may be expected to have a different behaviour in downstream processes (Aydogan et al., 2006). Previous studies have shown that the micro-fractures introduced into HPGR improve downstream separation process, such as heap leaching, flotation, and gravity (Esna-Ashari and Kellerwessel, 1988; Baum et al., 1997; Palm et al., 2010; Solomon et al., 2010; Chapman et al., 2013; Ghorbani et., 2013). A paper by Gens et al. (2008) provided quantitative data on the benefit of crushing the clinker feed in an HPGR prior to the ball mill. The circuit capacity was increased by 10% and the specific energy was reduced by 9.1%.

The aim of this study is to study and compare the effect of HPGR and conventional crushing on the grinding kinetics of downstream ball milling of an iron ore.

Experimental

Material

The samples used in this research were obtained from the Jalalabad Iron Ore Mine in Kerman Province, Iran. In the Jalalabad Iron Ore Plant, the mined ore is crushed in a primary gyratory crusher and then the crushing product is fed to a HPGR. For comparative purposes, two samples were taken from the feed stream and product stream of HPGR. The HPGR feed sample was further crushed by a laboratory jaw crusher and cone crusher. The overview of the sample preparation used for this study is summarized in Fig. 1. The jaw and cone crushers were adjusted in such a way that the conventional crushers and HPGR products had similar size distribution. Figure 2 shows the size distribution of the products. Products from the conventional crushers and HPGR were then screened into five single-sized fractions: (–4+3.15 mm), (–2+1.7 mm), (–1+0.850 mm), (–0.500+0.420 mm), and (–0.212+0.180 mm). One sample with 300 g weight was prepared from each fraction.

Mineralogy

For mineral investigation, three lumps of ore were selected and studied by Zeiss Axioplan2 research optical microscope. Mineralogical analysis revealed that the sample consisted of magnetite (0.1-0.8 mm) with minor content of pyrite (0.2-3.5 mm) and trace of chalcopyrite (<0.3 mm). Quartz, calcite, chlorite, talc, and dolomite were the major nonmetallic minerals, which mainly filled the spaces around magnetite crystals. The main texture of ore was massive with a sign of tectonic compressions, which caused a shattered texture in subsamples (Fig. 3).

In order to check the general mineralogy, semi quantitative XRD examinations were carried out on the representative sample (Table 1). Based on the XRD examination, magnetite and hematite were the major and minor ore minerals, respectively. Talc, chlorite, and quartz were the major gangue in the ore sample.

Grinding test

Grinding tests were performed in a 20 cm×20 cm stainless steel laboratory mill. It was operated at the constant speed of 85 rpm (84% of the critical speed). The mill charge consisted of stainless steel balls with 16–42 mm diameter and the total ball load weighing 8.79 kg. The ball voids were 43.33% of the volume of the ball charge. The volume of the ball charge with voids was 25% of the total volume of the mill. The fraction of ball charge filled by powder was 0.27. Each fraction of the ore was ground individually and batch wise for a short time period until about 50% of the material was passed through the top screen. For better measurement of the breakage rate (S value), grinding was continued until about 90% of the material passed through the top screen. After the grinding test of each size fraction in varying grinding periods, the mill content was discharged and sieved for 20 min using the stack of ($\sqrt{2}$) spaced sieves to determine size distributions.
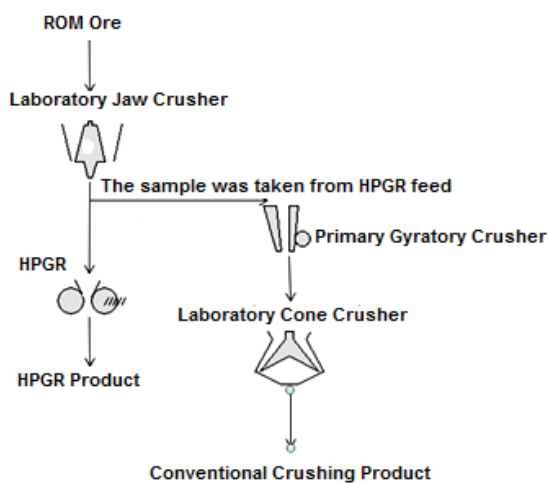

Fig. 1. Procedure used for sample preparation

Also, for verifying the results, two samples of 665 g in weight and the same size distribution were manually made from the HPGR and crusher products and ground under the same condition for different time periods.
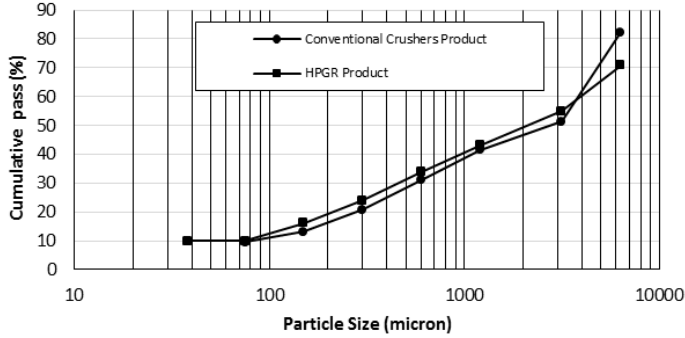

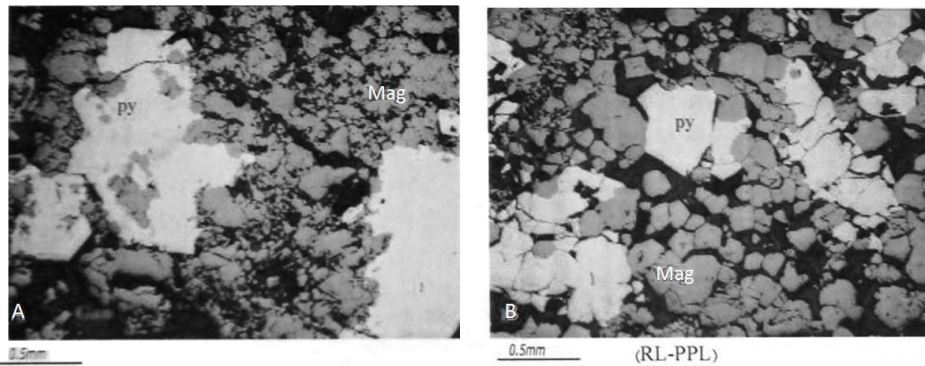Fig. 2. Particle size distribution of HPGR and conventional crushers

Fig. 3. Inclusions of magnetite in pyrite (A) and gangue mineral enveloped around magnetite grain (B)

Table 1. Semi-quantitative XRD mineralogy

Mineral Name	Formula	%
Magnetite	Fe_3O_4	38
Hematite	Fe_2O_3	7
Goethite	$FeO(OH)$	3
Pyrite	FeS_2	3
Chalcopyrite	$CuFeS_2$	0.5
Talc	$Mg_6(Si_8O_{20})(OH)_4$	16
Chlorite	$(Mg,Al,Fe)[(Si,Al)_8O_{20}](OH)_{16}$	10
Quartz	SiO_2	10
Calcite	$CaCO_3$	8.5
Dolomite	$CaMg(CO_3)_2$	4

Results and discussion

Determination and comparison of cumulative breakage distribution function

Cumulative breakage distribution function, $B_{i,1}$, was estimated from the size analysis of the product from short-time grinding of starting mill charge predominantly at size j by modified Herbst and Furestenau (1968) method Eq. (1).

$$B_{i,1} = \frac{\text{Ln}[1 - Y_i(t)]}{\text{Ln}[1 - Y_1(t)]} \qquad i \geq 1 \tag{1}$$

where $Y_i(t)$ is the cumulative percentage of the broken materials, passing from size x_i at time t. Obviously, $Y_1(t)$ is the cumulative percentage of the broken materials passing from size x_1 at time t. By plotting $\text{Ln}[1 - Y_i(t)]$ values versus $\text{Ln}[1 - Y_1(t)]$ values, a straight line is obtained where $B_{i,1}$ is the slope of the line. Good results were obtained when the time of grinding was chosen to give an amount of material broken out of the top size interval of about 20–30%. The values of cumulative breakage distribution function can be closely fitted by Eq. (2) (Austin et al., 1984).

$$B_{i,1} = \varphi R^\gamma + (1 - \varphi)R^\beta \qquad i \geq 1 \tag{2}$$

where R is relative size ($R = \frac{x_i}{x_1}$) and φ, γ, and β are the characteristic of the material being ground and define the size distribution. These parameters can be experimentally determined by plotting $B_{i,1}$ values versus relative size (R) on log–log scales (Fig. 4). The slope of the lower straight-line part of the curve gives the value of γ, the slope of the upper part of the curve gives the value of β, and φ is the intercept (Austin et al., 1984). The value of γ is related to the relative amount of fines produced while β and φ are related to the coarse end of the breakage distribution function and show how fast fractions close to the feed size pass to a smaller size interval.

Figure 4 shows the $B_{i,1}$ curve for all single sized fractions. It can be seen that all the fraction $B_{i,1}$ values for the HPGR product were higher than those of the crusher product. It means that the progeny particles produced from dry ball milling of the HPGR product were finer than from the crusher. Parameters β, γ and φ were obtained from the $B_{i,1}$ curve by fitting (Eq. 2) to the experimental data illustrated in Fig. 4. As a rule of thumb, for an optimal fitting, the number of parameters was reduced by assuming parameter β constant for normal breakage. The value of (β) was taken from the literature ($\beta = 3.5$; Austin et al., 2007, Koleini and Barani, 2012). Therefore, in this case, the sensitivity of only two parameters (γ and φ) was investigated.

The determined breakage distribution parameters with the corresponding feed particle sizes for both crusher and HPGR conditions are listed in Table 2. Data presented in Table 2 indicate a noticeable decrease in γ parameter for the HPGR. It can be seen that the HPGR affected the value of γ parameter at coarse particles and decreased at fine particles. Relative difference between the value of γ at (–4+3.15mm) fraction was 27%. A higher value of γ implied that the progeny fragments were

coarser, i.e. their size was closer to the size of the parent material being broken and that grinding took place at a slow rate (Makokha and Moys, 2006). On the contrary, a lower value of γ would imply more effective breakage action with high production of fine particles. In general, softer materials would display lower values of γ as compared with harder materials.
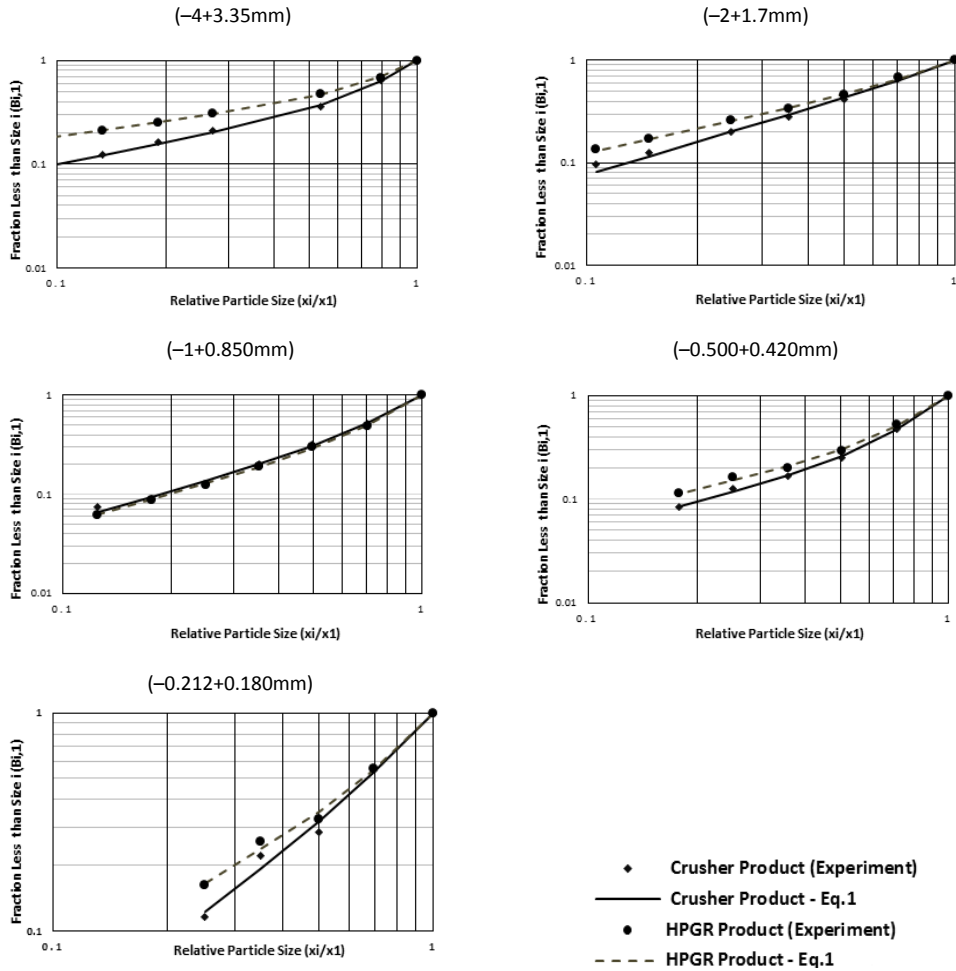

Fig. 4. Cumulative breakage distribution function for all single sized fractions

Determination and comparison of specific rate of breakage

In the analysis of the breakage of materials, it is useful to assume that the breakage of each size fraction is of first order in nature (Austin, 1972)

$$w_1(t) = w_1(0)exp(-S_1t) \tag{3}$$

That is

$$log(W_1(t)) = log(W_1(0)) - \frac{S_1 t}{2.3} \tag{4}$$

where $W_1(0)$ and W_1 (t), respectively, are the weight fractions of the top size fraction at times 0 and t and S_1 is a proportionality constant called the specific rate of breakage with unit of time^{-1}. This equation denotes that $(\frac{W_1(t)}{W_1(0)})$ versus t should give a straight line on log-linear coordinates and S_1 can be determined from the slope of the line.

Table 2. Breakage distribution parameters ($\beta = 3.5$)

Fraction		γ	φ
−4+3.15mm	HPGR	0.487	0.562
	Crusher	0.669	0.469
−2+1.7mm	HPGR	0.808	0.793
	Crusher	1.072	0.898
−1+0.850mm	HPGR	1.004	0.502
	Crusher	1.037	0.566
−0.500+0.420mm	HPGR	0.788	0.436
	Crusher	0.841	0.360
−0.212+0.180mm	HPGR	0.968	0.626
	Crusher	1.296	0.727

Figure 5 shows the plots obtained from one-size fraction tests. Good first-order kinetics were obtained for all the fractions, except the coarsest fraction (−4+3.15 mm, Fig. 5), which is a typical result for a feed that has some too large particles to be nipped by the ball size in the mill. Thus, the rate of breakage is less than the expected value and decreases as grinding proceeds, probably due to the accumulation of the harder (stronger) material in the remaining feed material (Austin et al., 2007). The results showed that the specific breakage rate of the material crushed by the HPGR at coarse fractions (−4+3.15 mm, −2+1.7 mm, and −1+0.850 mm) was higher than the material crushed by the conventional crushers. However, at fine fractions (−0.500 +0.420 mm and −0.212+0.180 mm), there is small difference and the specific breakage rates were the same. Relative difference between S value for (−4+3.15 mm) and (−0.212+0.180 mm) fractions was 54% and 2%, respectively. Figure 6 shows the variation of S_i values against feed particle sizes. It can be seen that, for the crusher product, the values sharply increased until 1.7 mm and then decreased. This means that there was optimum feed size (about 1.7 mm) where the greatest breakage occurred. This issue can be explained by the fact that large particle sizes were difficult to be reduced and ground by the medium. So, the grinding efficiency had to be

decreased, while for the HPGR product, the greatest breakage rate occurred at 3.15 mm. HPGR crushing increased the breakage rate of iron ore, especially at coarse fractions. At coarse fractions, the particles had longer side surfaces and thus were more affected by lateral pressure.
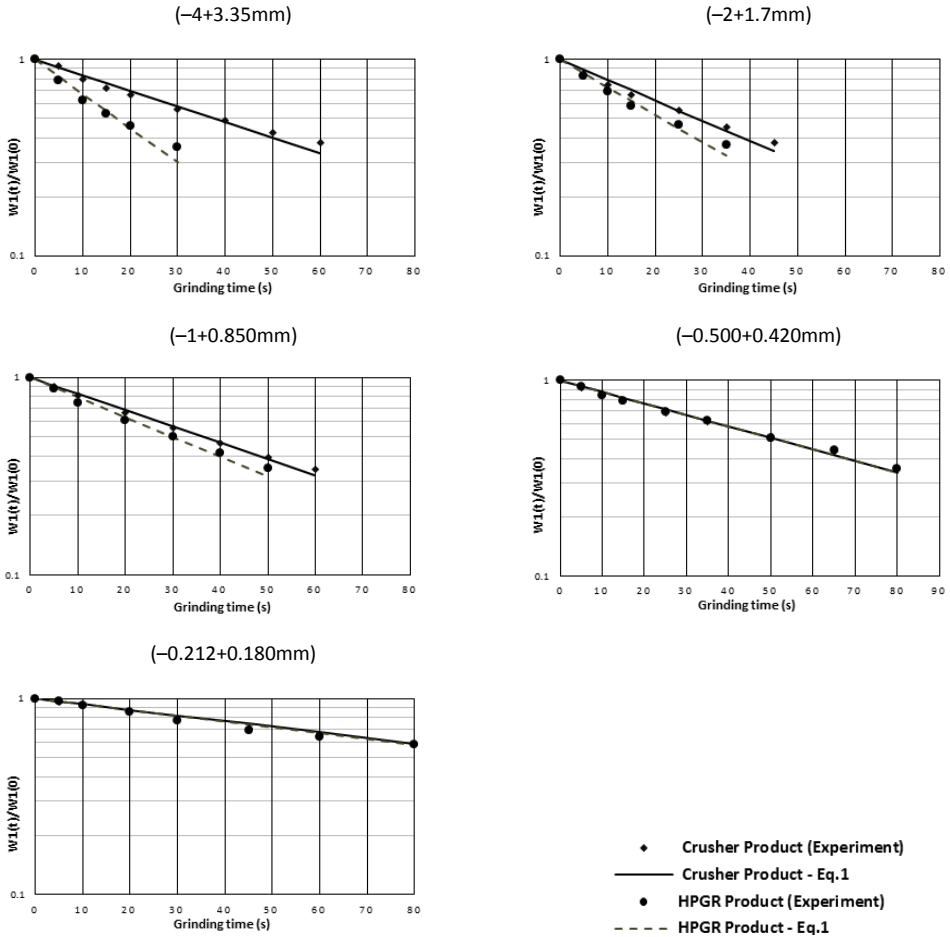

Fig. 5. First-order plot for batch dry grinding of all single sized fractions

Verification of results

For verifying the results, two samples with 665 g weight and the same size distribution were manually made from the HPGR and crusher products and ground under the same condition for different grinding time periods. Figure 7 shows the size distribution of the crusher and HPGR products after grinding. It can be seen that, in all the grinding periods, the HPGR product produced a finer ground product. Figure 8 shows P_{80} (80% passing size) variation versus grinding time. After 60 s of dry ball mill grinding, P_{80} of the crusher and HPGR products was 1267 and 760 micrometer, respectively. With

increasing grinding time to 120 s, this difference was decreased. However, with increasing grinding time, the percent passing 180 micrometer was increased more rapidly for the HPGR product compared to the crusher product. After 120 s of grinding, the percent passing 180 micrometer was 56% and 51%, respectively, for the HPGR product and crusher products. These results verify and confirm the results of breakage and selection function tests and show pre-crushing by the HPGR produces softer feed for ball mill grinding.

The crusher and HPGR products were ground under the same condition and time. Then, the work indices of the samples can be determined by the Berry and Bruce comparative grind ability method (Berry et al., 1966). If C is the crusher product and H is the HPGR product, from the Bond equation:

$$W_C = W_H = 11 Wi_C \left[\frac{1}{\sqrt{P_C}} - \frac{1}{\sqrt{F_C}} \right] = 11 Wi_H \left[\frac{1}{\sqrt{P_H}} - \frac{1}{\sqrt{F_H}} \right]. \tag{5}$$

Therefore,

$$\frac{Wi_H}{Wi_C} = \frac{\left[\frac{1}{\sqrt{P_C}} - \frac{1}{\sqrt{F_C}} \right]}{\left[\frac{1}{\sqrt{P_H}} - \frac{1}{\sqrt{F_H}} \right]} \tag{6}$$

where W is energy consumption (kWh/Mg), W_i is Bond work index, and F and P are 80% passing size of feed (μm) and product, respectively.

The work index of HPGR product to crusher product $\frac{Wi_H}{Wi_C}$ was determined by the Berry and Bruce method and presented in Fig 8. It shows that at the early grinding time, where large particles were ground preferably, there was a large difference between indices and the ratio of $\frac{Wi_H}{Wi_C}$ was low, because, as mentioned above, large particles were more affected by HPGR. With increasing grinding time, the ratio of $\frac{Wi_H}{Wi_C}$ was increased.
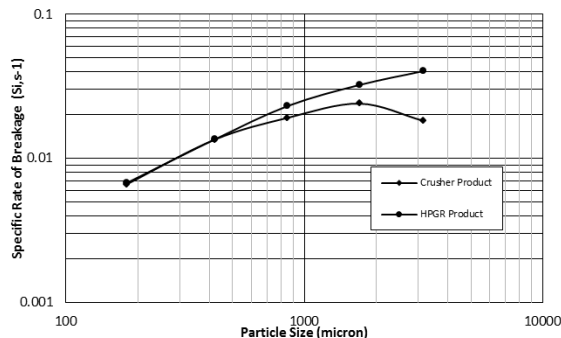

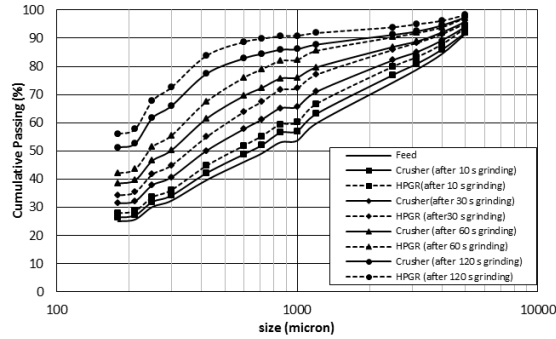Fig. 6. Specific rates of breakage of ore versus particle size (WSSE, weighted sum squared errors)

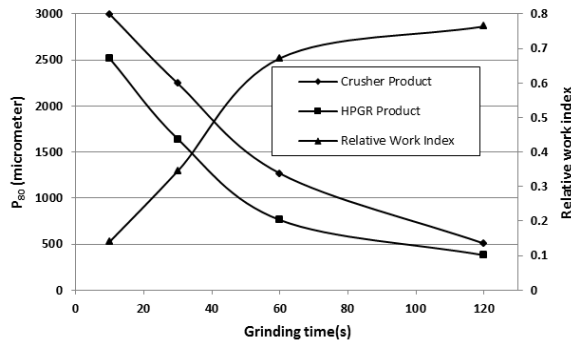Fig. 7. Size distribution of the same feed and grinding products

Fig. 8. The variation of HPGR and crusher P_{80} and relative work index ($\frac{Wi_H}{Wi_C}$) with grinding time

Conclusions

The aim of this study was to verify and compare the effect of the HPGR and conventional crushing on the grinding kinetics of downstream ball milling of an iron ore. It was found that all the fraction cumulative breakage function values ($B_{i,1}$) for the HPGR product were higher than those for the crusher product. It means that progeny particles produced from the dry ball milling of HPGR product were finer than the crusher. Also, all the fraction γ values for the HPGR product were lower than those for the crusher product, especially at coarse fractions. In general, softer materials would display lower values of γ as compared with harder materials. Relative difference between value of γ at (–4+3.15mm) fraction was 27%.

An analysis of the breakage rate tests showed that the specific breakage rate of the material crushed by HPGR at coarse fractions (–4+3.15 mm, –2+1.7mm, and –1+0.850mm) was higher than the material crushed by the conventional crushers. However, at fine fractions (–0.500+0.420 mm and -0.212+0.180 mm), there was small difference and the specific breakage rates were the same. The relative difference between S value for (–4+3.15 mm) and (–0.212+0.180 mm) fractions was 54% and

2%, respectively. In the HPGR, the particles were broken by compression in a packed particle bed and coarse particles had longer side surfaces and thus were more affected by lateral pressure. The results of test verification demonstrated that, after 60 s grinding, the 80% passing size of the HPGR and crusher products (D_{80}) respectively were reduced from 3311 μm to 761 μm and 1267 μm.

It can be concluded that the HPGR crushing, compared to the conventional crushing, increased the breakage rate of iron ore, especially at coarse fractions and produced softer feed for ball mill grinding.

Acknowledgment

References

AUSTIN L. G., JULIANELLI K., SCHNEIDER C. L., 2007, *Simulation of wet ball milling of iron ore at Carajas, Brazil*, International Journal of Mineral Processing, 84, pp. 157–171.

AUSTIN L. G., JULIANELLI K., SCHNEIDER C. L., 2007, *Simulation of wet ball milling of iron ore at Carajas, Brazil*, International Journal of Mineral Processing, 84, pp. 157–171.

AUSTIN, L. G., 1972, *A review introduction to the mathematical description of grinding as rate process*, Powder Technology, 5, pp. 1–17.

AUSTIN, L. G., KLIMPEL, R. R., LUCKI, P. T., 1984, *Process Engineering of Size Reductions*, Chapter 9, In Methods for Direct Experimental Determination of the Breakage Functions, New York: SME-AIME.

AYDOGAN, N.A., ERGUN, L., BENZER, H., 2006, *High pressure grinding rolls (HPGR) applications in the cement industry*. Minerals Engineering 19 (2), 130–142.

BAUM W., PATZELT N., KNECHT J., 1997, *Metallurgical benefits of high pressure roll grinding for gold and copper recovery*, SME, Denver, Feb. 1977. Conference print, pp.111-116.

BEARMAN R., 2006. *High-pressure grinding rolls: characterizing and defining process performance for engineers,* Advances in Comminution Komar Kawatra, S. (ed.). Society for Mining, Metallurgy and Exploration, Denver, Colorado. pp. 3–14.

BERRY, T.F., BRUCE, R.W., 1966, A Simple Method for Determining the Grindability of Ores. Canadian Mining Journal, Vol 6, 6, 1966, pp. 385-387.

CHAPMAN N.A., SHACKLETON N.J., MALYSIAK V., O'CONNOR C.T., 2013, *Comparative study of the use of HPGR and conventional wet and dry grinding methods on the flotation of base metal sulphides and PGMs*, The Journal of The Southern African Institute of Mining and Metallurgy, Vol 113, pp.407-413.

DANIEL M.J., 2007, *Energy efficient mineral liberation using HPGR technology*, PhD thesis, University of Queensland, Brisbane, Australia.

DUNNE R., GOHLSBRA A., DUNLOP I., 1996, *High pressure grinding rolls and the effect on liberation: comparative test results*, Proceedings of Randol Gold Forum. Randol International, Golden, Colorado. pp. 49-54.

ESNA-ASHARI M., KELLERWESSEL H. 1988, *Roller press comminution improves heap leach recovery*. Randol Perth International Gold Conference, Perth 28 October – 1 November 1988. pp. 50-53.

GENS A.H., BENZER S.L., ERGUN S.L., 2008, *Effect of High Pressure Grinding Rolls (HPGR)on performance of two-compartment cement ball mill*. 11th International Mineral Processing Symposium, Belek-Antalya, Turkey, p. 69.

GHORBANI A., MAINZA A.N., PETERSEN J., BECKER M., FRANZIDIS J-P., KALALA J.T., Investigation of particles with high crack density produced by HPGR and its effect on the redistribution of the particle size fraction in heaps, Minerals Engineering 43–44 (2013) 44–51.

HERBST J.A. , FUERSTENAU D.W., 1968, *The zero order production of fine size in comminution and its implication in simulation*, Trans. SME, AIME, Vol. 241, pp. 538-548.

KELLERWESSEL H., 1990. *High-pressure material-bed comminution in practice*. Translation ZKG 2 (90), 57–64.

KLYMOWSKY R., PATZELT N., KNECHT J., BURCHARDT E., 2006, *An overview of HPGR technology.* International autogenous and semiautogenous grinding technology. Proceedings of the SAG conference. Allan, M.J. (ed.). Department of Mining Engineering, University of British Columbia.Vancouver, BC, Canada. pp.11-26.

KOLEINI S.M.J., BARANI K., REZAEI B., 2012, T*he effect of microwave treatment upon dry grinding kinetics of an iron ore*, Mineral Processing and Extractive Metallurgy Review Journal, vol. 33 (2), pp.159-169.

MAKOKHA A., MOYS M. H., 2006, *Towards optimizing ball-milling capacity: Effect of lifter design*, Minerals Engineering, 19, pp. 1439–1445.

MORLEY C., 2006. *High pressure grinding rolls: a technology review*. Advances in Comminution. Komar Kawatra, S. (ed.). Society for Mining, Metallurgy and Exploration, Denver, Colorado. pp. 15–39.

PALM N.A., SHACKLETON N.J., MALYSIAK V., O'CONNOR C.T., 2010, *The effect of using different comminution procedures on the flotation of sphalerite*. Minerals Engineering. 23, pp. 053–1057.

SCHNEIDER L.C., ALVES K.V., AUSTIN G.L., 2009. *Modelling the contribution of specific grinding pressure for the calculation of HPGR product size distribution*. Minerals Engineering 22, 642–649.

SCHONERT K., 1979, *Aspects of the physics of breakage relevant to comminution*, Fourth Tewksbury Symposium, University of Melbourne 3(1), pp. 3.30.

SCHONERT K., KNOBLOCH O., 1984. *Energetische Aspekte des Zerkleinerns Sprö der Stoffe Zement-Kalk-Gips*, 37 (11), 563–568.

SCHONERT K., 1988, *First survey of grinding with high-compression roller mills*. International Journal of Mineral Processing 22, 401–412.

SOLOMON N., BECKER M., MAINZA A., PETERSEN J., FRANZIDIS J.-P., 2010, *Understanding the influence of HPGR on PGM flotation behavior using mineralogy*, Minerals Engineering 24, pp.1370–1377.